Separation and Purification Technology 364 (2025) 132608

Contents lists available at ScienceDirect

Separation and Purification Technology

journal homepage: www.elsevier.com/locate/seppur

High-capacity nonwoven increases productivity of mAb purification in an all-membrane process

Jinxin Fan [a,*], Joseph Lavoie [b], Jacob LeBarre [a], Stefano Menegatti [a,b], Behnam Pourdeyhimi [a,c], Cristiana Boi [a,b,d,**], Ruben G. Carbonell [a,b,e]

[a] Department of Chemical and Biomolecular Engineering, North Carolina State University, Raleigh, NC 27695-7905, USA
[b] Golden LEAF Biomanufacturing Training and Education Center (BTEC), North Carolina State University, Raleigh, NC 27695-7905, USA
[c] Nonwovens Institute, North Carolina State University, Raleigh, NC 27695-7905, USA
[d] DICAM, Alma Mater Studiorum-Università di Bologna 40131 Bologna, Italy
[e] National Institute for Innovation in Manufacturing Biopharmaceuticals (NIIMBL), Newark, DE 19711, USA

ARTICLE INFO

Editor: Raquel Aires Barros

Keywords:
Multimodal anion exchange
Membrane adsorber
Membrane chromatography
Nonwoven membrane
monoclonal antibodies (mAbs)

ABSTRACT

There is significant interest in alternative manufacturing processes for monoclonal antibodies (mAbs) to improve productivity and reduce cost. To identify a cost-effective and high-productivity alternative to the conventional Protein A-based mAb capture step, this study presents the development of a high-performance multimodal anion exchange (MMA) membrane utilizing N-Benzyl-N-methylethanolamine (BMEA) as the ligand which was covalently coupled to a polyglycidyl methacrylate (pGMA) UV-grafted polybutylene terephthalate (PBT) nonwoven. The $DBC_{10\%}$ of the MMA membrane for IgG ranged from 32.8-42.4 mg/mL at 0.5 to 5 min residence time. The membrane exhibited an excellent salt tolerance in protein binding near physiological conditions, high flow permeability and good reusability. The MMA membrane also showed a $DBC_{10\%}$ of 59.2 mg/mL for direct capture of a mAb from a CHO supernatant without the need for pH or conductivity adjustments, along with a recovery of 94.3%, a 1.0 log reduction value (LRV) of host cell proteins (HCPs), a 1.8 LRV for DNA, and a reduction of aggregates from 5.4% to 0.9%. This capture step was implemented in an all-membrane mAb purification process that included a viral inactivation step and two polishing steps using an anion exchange nonwoven (AEX-TEA) and a multimodal cation exchange nonwoven (MMC-MPCA). A side-by-side comparison with a platform mAb purification process using Protein A resin and two ion exchange resins showed that the all-membrane process exhibited similar impurity clearance, higher overall recovery (88.3% vs. 77.5%) and significantly reduced processing time (3.8 h vs. 13.1 h) with fewer steps as it eliminates the need for diafiltration for buffer exchange.

1. Introduction

Therapeutic monoclonal antibodies (mAbs) are the dominant biopharmaceutical class in terms of both the numbers of approvals and sales [1]. They have been broadly applied in the treatment of cancers, rheumatoid arthritis, multiple sclerosis, autoimmune disorders, and COVID-19 [2,3]. However, the costs associated with such treatment impose a significant financial burden on patients and healthcare systems [4]. To improve their accessibility and affordability, biopharmaceutical companies have invested considerable resources in transforming mAb manufacturing processes to enhance productivity, reduce capital and operating costs, and decrease turnaround times [5,6]. Downstream processing, which accounts for over 50% of mAb production costs, typically relies on platform processes requiring two or three-step resin chromatography operations involving a Protein A chromatography product capture step and one or two subsequent ion exchange chromatography steps for polishing [7,8]. However, Protein A resins contribute over 50% of the total downstream processing cost; they are susceptible to ligand leaching, and the low pH elution steps can cause mAb aggregation. Even though the resins can be used in over 100 cycles of operation, they require cleaning and sanitization in strong alkaline solutions [9,10]. As a result, considerable attention has been directed towards the development of alternative non-Protein A processes, including precipitation [11,12], aqueous two-phase extraction [13,14],

* Corresponding author.
** Corresponding author at: Department of Chemical and Biomolecular Engineering, North Carolina State University, Raleigh, NC 27695-7905, USA.
E-mail addresses: jfan22@ncsu.edu (J. Fan), cboi@ncsu.edu (C. Boi).

https://doi.org/10.1016/j.seppur.2025.132608
Received 1 February 2025; Received in revised form 10 March 2025; Accepted 17 March 2025
Available online 19 March 2025
1383-5866/© 2025 The Author(s). Published by Elsevier B.V. This is an open access article under the CC BY-NC license (http://creativecommons.org/licenses/by-nc/4.0/).

mixed-mode chromatography [15,16], and peptide-based affinity chromatography [17].

Multimodal or mixed-mode chromatography relies on a combination of different intramolecular forces to bind mAbs to resins or membranes and can achieve high purity and yield of the resulting product with optimized pH, conductivity and specific salts and other additives used in the binding, wash and elution steps [10,16,18]. Multimodal ligands typically demonstrate salt-tolerance [19,20], reducing the need for buffer exchange or dilution prior to protein binding – a step that is usually required in conventional ion exchange chromatography that increase process times and operating costs [21,22]. Multimodal cation exchange (MMC) chromatography of mAbs requires an operating pH (usually 4.5–6.0) that is lower than the pI of most mAbs (generally between 6.1 and 9.4) [16,23]. Multimodal anion exchange (MMA) chromatography can operate in conditions that closely resemble physiological conditions, where the ligand remains positively charged, and it has the potential to enable the direct capture of mAbs at pH values close to the pI of the mAb. As examples the performance of the four principal MMA resins (Capto^{TM} adhere, PPA HyperCel, HEA HyperCel and MEP HyperCel) currently available on the market depend on the charges and hydrophobicities of the ligands, as well as their interactions with impurity proteins exhibiting distinct surface charge distributions and hydrophobic zones [24,25]. While multimodal ligands on chromatographic resins are known to be effective in impurity removal, the reported binding capacity of MMA resins for mAb capture from the supernatant (titers in the range of 0.4–1.69 mg/mL) have been found to be generally low (<20 mg/mL with residence time of 2.5–6.6 min), resulting in low productivity [24–26].

A variety of chromatographic membranes based on microporous and fibrous materials have been employed in the high-throughput purification of biologics [27–29]. Membrane systems are typically single-use-devices that offer significant savings in overall processing costs and relatively short residence times. Membranes provide alternatives to resin chromatography with higher productivity and lower capital expenditures for the capture of mAbs, separation of charged variants, and clearance of HCPs, DNA and aggregates [5,30–32]. However, to our knowledge, only one MMA microporous membrane has been reported in the literature, which was applied for the clearance of HCP and aggregate impurities in mAb polishing processes [30]. As far as the authors are aware, the work described in this paper is the first reported application of an MMA membrane in mAb product capture, in the context of an all-membrane process platform.

The objectives of this study are: (1) to develop a high-capacity MMA membrane for direct mAb capture from a cell culture supernatant, and: (2) to compare the performance of an all-membrane non-Protein A purification process for mAbs from CHO cell culture to the performance of a traditional resin chromatographic platform process. Inexpensive nonwoven fabrics are a promising class of materials that exhibit low pressure drops at high flow rates and can be used as the base for high-throughput, high-capacity disposable chromatographic membranes [32–35]. This effort relies on prior studies using polybutylene terephthalate (PBT) nonwoven fabrics functionalized with ion-exchange or multimodal ligands for the purification of mAbs and single-chain antibody fragments (scFv) [20,36,37]. The relatively large pores on these membranes and the ability of the grafted layer to accommodate several layers of bound proteins enabled short residence times and high dynamic binding capacities at residence times of less than one minute. As an example, the iminodiacetic acid (IDA)-PBT nonwoven exhibited a $DBC_{10\%}$ of 76.6 mg hIgG/mL at 0.1 min residence time [37,38].

In the present study, a polyglycidyl methacrylate (pGMA) grafted PBT nonwoven fabric was employed to prepare an MMA membrane through the conjugation of N-Benzyl-N-methylethanolamine (BMEA) to pGMA. It was anticipated that the resulting membrane with ion exchange and hydrophobic groups in the BMEA ligand, would exhibit a good salt tolerance and protein binding capacity for direct mAb capture at a relatively short residence time. The influence of ligand density on the performance of the MMA-BMEA membranes was first investigated by measuring the static binding capacity (SBC) for bovine serum albumin (BSA), a model protein utilized for preliminary characterization of anion exchange materials. The flow permeability and the impact of salt concentration on dynamic binding capacity (DBC) of the membrane were also studied. The $DBC_{10\%}$ for BSA measured at varied RTs was then compared to that of a commercial MMA resin (Capto^{TM} adhere) under the same conditions. The $DBC_{10\%}$ and isotherm for IgG binding to the MMA-BMEA membrane, along with its reusability in five consecutive IgG bind-and-elute cycles, were studied to evaluate its performance for antibodies.

Subsequently, the MMA-BMEA membrane was used for the capture of a mAb from a CHO cell culture fluid in an all-membrane process that included viral inactivation and polishing steps. The performance of the MMA-BMEA membrane at different RTs, wash and elution conditions, was investigated in terms of product recovery and impurity removal. The polishing steps included use of an anion exchange nonwoven membrane with triethylamine as ligand (AEX-TEA) in a flowthrough mode after the viral inactivation step. A final polishing step included the use of a multimodal cation exchange nonwoven membrane with 2-mercaptopyridine-3-carboxylic acid as ligand (MMC-MPCA) in a bind-and-elute mode. The results were then compared with those of a standard three-step resin chromatography process, which comprised a Protein A capture step, a virus inactivation step, and subsequent cation exchange and anion exchange chromatography for polishing (Fig. 1). The results indicate that all-membrane processes can result in significant improvements in overall productivity and no losses in product quality.

2. Experimental

The three-step all-membrane chromatography process was carried out with three different nonwoven membranes: (1) an anion exchange nonwoven membrane with triethylamine as ligand (AEX-TEA), (2) a multimodal cation exchange nonwoven membrane with 2-mercaptopyridine-3-carboxylic acid as ligand (MMC-MPCA) described previously [20,35], and (3) the new MMA-BMEA membrane described in this work. This paper first describes the preparation and preliminary characterization of the MMA-BMEA membrane and then focuses on the all-membrane mAb purification process and its comparison with the platform process utilizing resin column chromatography.

2.1. Materials

Polybutylene terephthalate (PBT) nonwoven membranes were provided by Macopharma (Tourcoing, France). This PBT nonwoven has the following properties: basis weight 55 g/m^2, fiber diameter 1.5–8.2 μm (mean fiber diameter: 3.0 μm), porosity 71%, and mean pore size 8.0 ± 0.5 μm. Glycidyl methacrylate (GMA) was purchased from Reagent World (Ontario, CA, USA). Benzophenone (BP), N-Benzyl-N-methylethanolamine (BMEA) and bovine serum albumin (BSA), Eshmuno® A resin and Amicon Ultra-15 Centrifugal Filter 10 kDa MWCO were purchased from Millipore Sigma (St. Louis, MO, USA). The organic solvents and chemicals used for membrane modification and buffers were purchased from Fisher Scientific (Fair Lawn, NJ, USA). Human polyclonal IgG (IgG) was purchased from Athens Research & Technology, Inc. (Athens, GA, USA). Omnifit^{TM} columns with 10 mm diameter were used as membrane holders and were purchased from Diba Industries, Inc., Cambridge, UK. The FPLC system ÄKTA pure^{TM}, 5 mm diameter empty columns (Tricorn 5/50) to pack chromatographic resin particles, Capto^{TM} adhere, Capto^{TM} Q and Capto^{TM} S resins were purchased from Cytiva (Marlborough, MA, USA). MMC-MPCA membrane and AEX-TEA membrane were prepared in our laboratory according to [20,35]. The Yarra SEC-2000 size exclusion chromatography column (3 × 7.8 mm) was purchased from Phenomenex Inc. (Torrance, CA, USA). The Waters Alliance 2690 separation module system and Waters 2487 dual absorbance detector for HPLC analysis were purchased from Waters

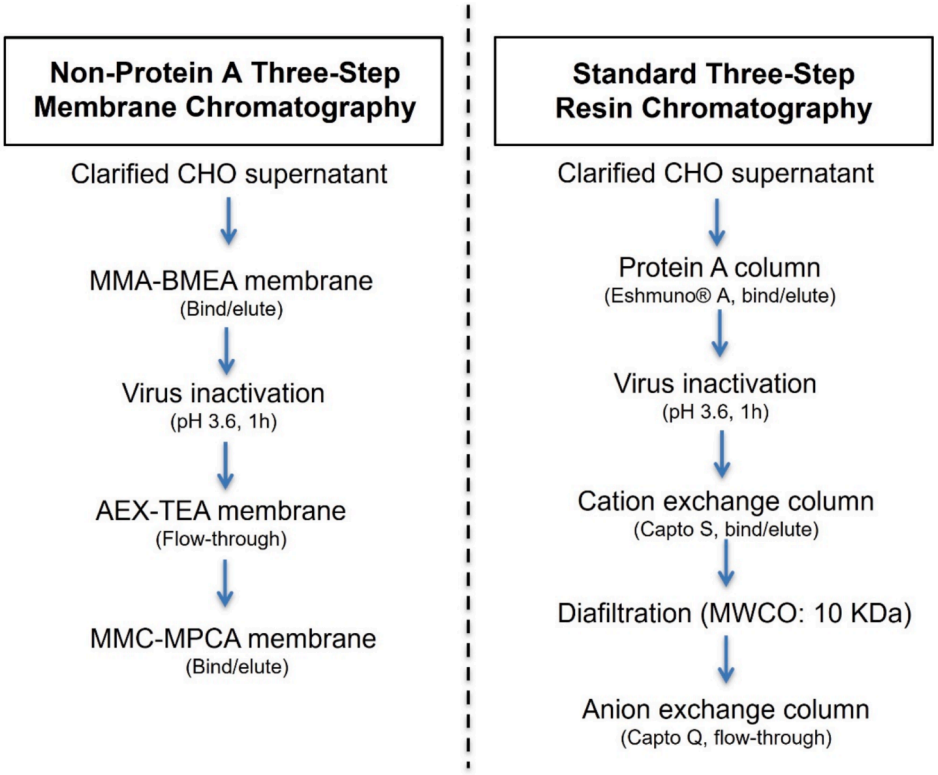

Fig. 1. Schematic diagram of non-Protein A three-step membrane chromatography and standard three-step resin chromatography containing Protein A for mAb capture.

Corporation (Milford, MA, USA). The CHO HCP ELISA Kit (F550-1) was purchased from Cygnus (Southport, NC, USA). Quant-iT™ PicoGreen™ dsDNA Assay Kit was bought from Fisher Scientific (Fair Lawn, NJ, USA). The CHO supernatant, containing 3.2 mg/mL of IgG_1 (mAb) pH 7.45 and conductivity 11.9 mS/cm, was generously provided by Fujifilm Diosynth Biotechnologies (Durham, NC, USA). The pI of this mAb is 7.6, very close to the pH of the supernatant.

2.2. Preparation of MMA-BMEA membrane

UV grafting of GMA on PBT nonwoven for ~ 20 min was conducted to obtain 20% weight gain polyGMA (the membrane weight increased up to 20% after grafting) using procedures previously described [36,37]. PolyGMA grafted PBT samples were soaked in BMEA solutions (2–15% v/v in 17% isopropyl alcohol/water v/v) for ligand coupling at 40°C in a water bath for 6 h, followed by 0.1 M sulfuric acid treatment at 50°C for 16 h to hydrolyze unreacted epoxy groups in polyGMA to diols. The prepared multimodal anion exchange membrane (MMA-BMEA membrane) was washed three times with pure water and stored in 20% ethanol/water v/v.

2.3. Membrane characterization

The ligand density was determined by analyzing the amine content of the functionalized membranes with a PE 2400 CHN elemental analyzer (PerkinElmer Inc., Waltham, MA, USA). A scanning electron microscope (SEM, Hitachi S-3200 N, Hitachi High-Tech, Schaumburg, Illinois, USA) was used to observe the morphology of the membrane surface (accelerating voltage: 5.0 kV). For flow permeability measurements, 48 layers of MMA-BMEA membrane were packed wet into a 10 mm diameter Omnifit™ column with a membrane bed height of 1.2 cm (0.94 mL column volume). Pressure drop (ΔP) was measured under various flow rates in an ÄKTA pure™ system using 50 mM Tris-HCl pH 7.0, with and without added 150 mM NaCl, as the mobile phase. At the flow rates under investigation the superficial velocities used were in the range 152.8–764.0 cm/h that correspond to 0.09–0.47 min residence times (RT). The ΔP across the membrane layers (kPa) was calculated by subtracting the pressure drop of the empty column from that of column with the membranes. The flow permeability of the membrane was calculated using Darcy's law:

$$v = k\frac{\Delta P}{\mu L} \tag{1}$$

Where v is the superficial velocity in the column, L is the height of membrane bed and μ is the viscosity of the aqueous solution.

2.4. Membrane performance for protein binding and elution

2.4.1. Elution optimization

Since the MMA-BMEA is a mixed-mode membrane, it is expected that the bound protein will not be completely eluted with NaCl alone, as is common in ion-exchange chromatography. Therefore, a study was performed to optimize the elution step using buffers with different pH values: 0.1 M citrate acid at pH 2.2, 50 mM glycine-HCl at pH from 3.0 to 3.5, and 50 mM acetate at pH from 4.0 to 5.0. In these experiments BSA was adsorbed on the membranes by immersing 15 mg of membrane samples (~0.05 mL) in 10 mg/mL BSA in 50 mM Tris-HCl pH 7.0 with 150 mM NaCl for 16 h at room temperature, then the recovery was calculated as the mass ratio of the eluted protein to the bound protein.

2.4.2. Batch equilibrium properties

The protein binding capacity at equilibrium (or static binding capacity) of the membrane was measured by protein binding to the membrane as described in 2.4.1, then elution was performed using 50 mM acetate buffer at pH 4.0. The binding capacity was calculated as the mass of eluted protein divided by the membrane volume. A range of IgG initial concentrations from 1.0 to 13.0 mg IgG/mL (dissolved in 50 mM

Tris-HCl pH 7.9 with added 120 mM NaCl) was employed for studying the equilibrium adsorption isotherm. The Langmuir isotherm was used to fit the experimental data:

$$q_{eq} = \frac{q_m c_{eq}}{c_{eq} + K_d} \quad (2)$$

Here q_{eq} is the measured amount of protein adsorbed on the membrane at equilibrium while c_{eq} is the protein concentration in the solution at equilibrium. The maximum binding capacity (q_m) and the dissociation constant (K_d) were determined by fitting the experimental data using Eq. (2).

2.4.3. Dynamic binding capacity

The dynamic binding capacity of the membrane at 10% breakthrough ($DBC_{10\%}$) was measured in flow experiments with 12 membrane layers (~0.24 mL membrane volume, 0.3 cm bed height) packed in the 10 mm diameter Omnifit™ column holder using the ÄKTA pure™ system. The membranes were equilibrated with 7.2 mL 50 mM Tris-HCl pH 7.0 with added 0–300 mM NaCl, and then 3 mg BSA/mL sample solution was loaded at 0.5 min, 1.0 min and 5.0 min RT. The sample loading was stopped once the UV absorbance reached the value corresponding to 10% of the initial feed concentration. The same procedure was used for 0.25 mL Capto™ adhere resin packed in a 5 mm diameter column for comparison. For measuring $DBC_{10\%}$ of MMA-BMEA membrane for IgG, 50 mM Tris-HCl pH 7.9 with added 120 mM NaCl was used as equilibration buffer and an IgG solution of 3.2 mg /mL was loaded at 0.5 min, 1.0 min, 2.0 min and 5.0 min RT. The $DBC_{10\%}$ was calculated as follows:

$$DBC_{10\%} = \frac{c_0(V_{10\%} - V_0)}{V} \quad (3)$$

where c_0 is the initial protein concentration in the feed (mg/mL); $V_{10\%}$ is the effluent volume when the protein concentration in the effluent reached 10% of the initial protein concentration in the feed (mL); V_0 is the void volume (mL) determined using a pulse of 2% acetone and V is the membrane or resin volume.

2.5. Membrane reusability evaluation

Five repeated bind and elute cycles of IgG binding were performed to evaluate reusability. 0.24 mL of membranes packed into the 10 mm diameter Omnifit™ column (0.3 cm bed height) were equilibrated with 7.2 mL of 50 mM Tris-HCl pH 7.9 with the addition of 120 mM NaCl (used as binding buffer), then 3.75 mL of IgG solution (3.2 mg/mL in binding buffer) was loaded to the membrane bed at 2 min RT. The membranes were washed abundantly with 7.2 mL binding buffer until the UV absorbance returned to baseline. The bound mAb was eluted with 7.2 mL 50 mM acetate pH 4.0, followed by membrane cleaning with 4.8 mL 0.5 M NaOH and re-equilibration with 12 mL binding buffer. The equilibration, washing, elution, cleaning and re-equilibration steps were all conducted at 0.5 min RT.

2.6. Purification of mAb from CHO supernatant with a three-step membrane process

2.6.1. First step: mAb capture with MMA-BMEA membrane

A 0.24 mL membrane bed packed in a 10 mm-diameter Omnifit™ column (0.3 cm bed height) was equilibrated with 7.2 mL 50 mM Tris-HCl pH 7.9 with added 120 mM NaCl at 0.5 min RT, then 7.5 mL of clarified CHO supernatant was loaded to the membranes at 2 min RT. The effluent was collected every 0.5 mL during sample loading and the mAb concentration was analyzed using a Protein G column according to [37]. The loading volume when the mAb concentration in the effluent reached 10% of the initial mAb concentration in the supernatant was used to calculate $DBC_{10\%}$ with equation (3). The membrane was then washed with the equilibration buffer and cleaned with 50 mM acetate pH 4.0. After the proper loading volume is determined (4 mL for loading), the effect of RT (0.5–5 min) for loading CHO supernatant and arginine concentration (50–125 mM) used in the wash step were studied. For further removal of impurities, a step pH elution of pH 4.5 and 4.0 was employed. The equilibration, washing and elution steps in the above runs were all conducted at 0.5 min RT. The final purification conditions for mAb capture with MMA-BMEA membrane are shown in Table 1.

2.6.2. mAb polishing: Second step in flow-through mode with AEX-TEA membrane, third step in bind-and-elute mode with MMC-MPCA membrane

The pH 4.5 eluate from the MMA-BMEA membrane step was adjusted to pH 3.6 by addition of 0.5 M HCl and incubated for 1.0 h at room temperature for virus inactivation. The resulting solution was then adjusted to pH 7.2 by 1.0 M Tris-HCl pH 8.0 and filtered using 0.22 μm membrane. The details of membrane equilibration, sample loading, washing and elution for mAb polishing by AEX-TEA membrane (flow-through mode) and MMC-MPCA membrane (bind-and-elute mode) are presented in Table 1. The membranes were packed in a 10 mm diameter column (~0.24 mL membrane volume, 0.3 cm bed height). The number of MVs (membrane volume) was used to record buffer volume. 0.5 M HCl and 0.5 M NaOH were used to adjust pH between each step. The membranes can be cleaned and regenerated with 0.5 M NaOH.

2.7. mAb purification by a standard three-step resin chromatography process

The resins were packed into a 5 mm diameter column (Tricorn 5/50) 0.28 mL Eshmuno® Protein A was used to capture mAb from the CHO supernatant, followed by virus inactivation using the same procedure as for the membrane process described in Section 2.6. The first polishing

Table 1
Details of chromatographic steps with nonwoven membranes.

Step	Buffer/Samples	Number of MVs	Residence Time (min)
A: MMA-BMEA Membrane (Bind/Elute)			
Membrane volume: 0.24 mL (ID = 10 mm, Bed Height = 3 mm)			
Equilibration	50 mM Tris-HCl + 120 mM NaCl, pH 7.9	20	0.5
Load	CHO supernatant	16.7 (4.0 mL)	2.0
Wash 1	50 mM Tris-HCl + 120 mM NaCl, pH 7.9	30	0.5
Wash 2	50 mM Tris-HCl + 100 mM Arginine, pH 7.4	30	0.5
Elution	50 mM acetate, pH 4.5	30	0.5
B: AEX-TEA Membrane (Flow-through)			
Membrane volume: 0.24 mL (ID = 10 mm, Bed Height = 3 mm)			
Equilibration	50 mM Tris-HCl, pH 7.2	20	0.25
Load	The eluate from MMA-BMEA after VI	10.4 (2.5 mL)	2.0
Wash	50 mM Tris-HCl, pH 7.2	30	0.25
Membrane cleaning	50 mM Tris-HCl + 1.0 M NaCl, pH 7.2	30	0.25
C: MMC-MPCA Membrane (Bind/Elute)			
Membrane volume: 0.24 mL (ID = 10 mm, Bed Height = 3 mm)			
Equilibration	50 mM acetate + 150 mM NaCl, pH 5.5	20	0.25
Load	The flow through fraction from AEX-TEA	14.6 (3.5 mL)	2.0
Wash 1	50 mM acetate + 150 mM NaCl, pH 5.5	20	0.25
Elution	50 mM sodium phosphate + 150 mM NaCl, pH 7.7	20	0.25

step, using 0.25 mL of Capto™ S resin, was performed in bind-and-elute mode. A 10 kDa centrifuge tube was used for buffer exchange to reduce the conductivity of the eluate prior to the next polishing step: 3.5 mL eluate was centrifuged at 3500 rpm for 30 min to reduce the volume to 0.25 mL, then 25 mM sodium phosphate buffer at pH 6.5 was added to make the final volume of 3.5 mL. The second polishing step with 0.25 mL Capto™ Q resin was conducted in flow-through mode. The three-step resin chromatography process was conducted at 5 min RT (4–6 min RT is commonly recommended). Details of the equilibration, sample loading, washing and elution steps are given in Table 2. The number of CVs (column volumes) was used to record the buffer volume. 0.5 M HCl and 0.5 M NaOH were used to adjust the pH between each step.

2.8. Analytics

The pure protein concentrations were determined using a UV–vis spectrophotometer at 280 nm with calibration curves based on known concentrations of the target protein. The mAb concentrations were measured using a 1 mL Protein G column according to [37]. The HCP and DNA levels were determined using the CHO HCP ELISA Kit (F550-1) and the Quant-iT™ PicoGreen™ dsDNA Assay Kit, respectively. The log reduction values (LRV) of HCP and DNA clearance were calculated as the $\log_{10}$ ratio of HCP (ppm) or DNA.

3. Results and discussion

3.1. MMA-BMEA membrane preparation

To construct a high-capacity multimodal anion exchange membrane for protein capture, a polyGMA-grafted PBT nonwoven fabric was prepared by UV irradiation, which enables the binding of several layers of protein to increase binding capacity. The epoxy groups on the grafted layer were used to link BMEA as a multimodal anion exchange ligand. Fig. 2 depicts the coupling of BMEA to the polyGMA grafted membrane by the reaction of the tertiary amine on the ligand and the epoxy group on the GMA [35,39,40]. The unreacted epoxy groups were then converted to diols using 0.1 M sulfuric acid. The BMEA ligand is expected to bind negatively charged proteins through the quaternary amine group under near physiological conditions. It can also bind near-neutral or uncharged proteins through hydrophobic and hydrogen-bonding interactions via the pendent phenyl and hydroxyl groups. These interactions are all expected to vary significantly with pH, conductivity, the presence of organic additives, the pI of the protein, and the ligand density on the grafted layer.

To study the role of ligand density and conductivity on protein binding, four MMA-BMEA membranes were prepared with different ligand concentrations in the solution during the coupling step ranging from 2% to 15% (v/v) and the membrane with the best protein binding ability was used for the subsequent studies.

The preliminary characterization of protein binding on the MMA-BMEA membrane was carried out using BSA, a model protein typically used to assess the performance of anion-exchange adsorbents as reported in the S.I. The membrane prepared with 15% v/v ligand solution achieved a high static binding capacity of 109.8 mg/mL and was selected for subsequent studies (**Fig. S1**). Further increases in the ligand concentration were not successful – a higher concentration of BMEA, 20% v/v, resulted in a pH higher than 13.5, which at the reaction temperature of 40°C for 6 h, cleaved some ester bonds in PBT, compromising the mechanical resistance of the membrane. Since the strong 0.1 M citric acid solution at pH 2.2 for elution can damage protein structure and potentially cause protein aggregation, we optimized the elution conditions and used 50 mM acetate at pH 4.0 as elution buffer in the subsequent studies (the results of elution pH optimization are shown in **Fig. S2**).

Table 2
Details of chromatographic steps with resins.

A: Protein A Resin (Eshmuno® Protein A, Bind/Elute)			
Resin volume: 0.28 mL (ID = 5 mm, Bed Height = 1.43 mm)			
Step	Buffer/Samples	Number of CVs	Residence Time (min)
Equilibration	PBS, pH 7.4	5	5.0
Load	CHO supernatant	14.3 (4.0 mL)	5.0
Wash 1	PBS, pH 7.4	10	5.0
Wash 2	25 mM sodium phosphate + 1.0 M NaCl, pH 7.2	10	5.0
Wash 3	25 mM sodium phosphate, pH 7.2	10	5.0
Elution	0.1 M glycine-HCl, pH 3.6	10	5.0
B: Cation Exchange Resin (Capto™ S, Bind/Elute)			
Resin volume: 0.25 mL (ID = 5 mm, Bed Height = 1.27 mm)			
Equilibration	50 mM acetate + 50 mM NaCl, pH 5.5	5	5.0
Load	The Protein A eluate after VI	20 (2.5 mL)	5.0
Wash	50 mM acetate + 50 mM NaCl, pH 5.5	10	5.0
Elution	50 mM acetate + 400 mM NaCl, pH 5.5	20	5.0
C: Anion Exchange Resin (Capto™ Q, Flow-through)			
Resin volume: 0.25 mL (ID = 5 mm, Bed Height = 1.27 mm)			
Equilibration	25 mM sodium phosphate, pH 6.5	5	5.0
Load	The eluate from Capto™ S	20 (2.5 mL)	5.0
Wash	25 mM sodium phosphate, pH 6.5	10	5.0
Elution	25 mM sodium phosphate + 1.0 M NaCl, pH 6.5	10	5.0

3.2. Flow characterization of MMA-BMEA membrane

High flow permeability properties of chromatographic membranes can reduce residence times and increase productivity. Since multimodal membranes or resins are usually able to operate under near physiological conditions, the flow permeability of the MMA-BMEA membrane was characterized using 50 mM Tris-HCl at pH 7.0 with or without 150 mM NaCl. Fig. 3 shows that the flow permeability of the MMA-BMEA membrane in these two buffers is 1.0×10^{-9} cm^2 and 4.6×10^{-9} cm^2, respectively. The charged grafted layer is expected to contract in the presence of high salt due to charge shielding with 150 mM NaCl. This results in larger effective pore diameters and a higher flow permeability. Due to the large inter-fiber distance of 3–40 μm as observed from SEM (**Fig. S3**), the flow permeability is higher than the permeabilities of commercial strong anion exchange resins with particle diameters of 50–90 μm (1.1×10^{-10} to 2.2×10^{-10} cm^2) [35]. The high flow permeability of the MMA-BMEA membrane results in low pressure drops, ΔP/L from 53.0 to 241.6 kPa/cm (0.64–2.95 bar for 1.2 cm bed) at 152.8 to 764.0 cm/h (RT from 0.47 – 0.09 min), well below the pressures (4–8 bar) of flow devices used in downstream processing.

The effect of NaCl concentration on the dynamic binding capacity ($DBC_{10\%}$) of the MMA-BMEA membrane for BSA was investigated at residence times (RT) of 1.0 and 5.0 min. A typical chromatogram for $DBC_{10\%}$ measurement at 1.0 min RT is shown in **Fig. S4**, while **Fig. S5** displays the results obtained at 1.0 and 5.0 min RT, both with 0 to 300 mM NaCl in 50 mM Tris-HCl pH 7.0. As the NaCl concentration increased from 0 to 300 mM, the $DBC_{10\%}$ of the MMA-BMEA membrane decreased from 49.1 to 17.9 mg BSA/mL at 1.0 min RT, and decreased from 61.0 to 20.9 mg BSA/mL at 5.0 min RT. Only 25%-35% of the binding capacity was lost at 150 mM compared to those measured without added NaCl at both RTs, indicating a good salt tolerance. The effect of charge screening by salt on protein adsorption was effectively offset by the role of hydrophobic interactions. The $DBC_{10\%}$ values

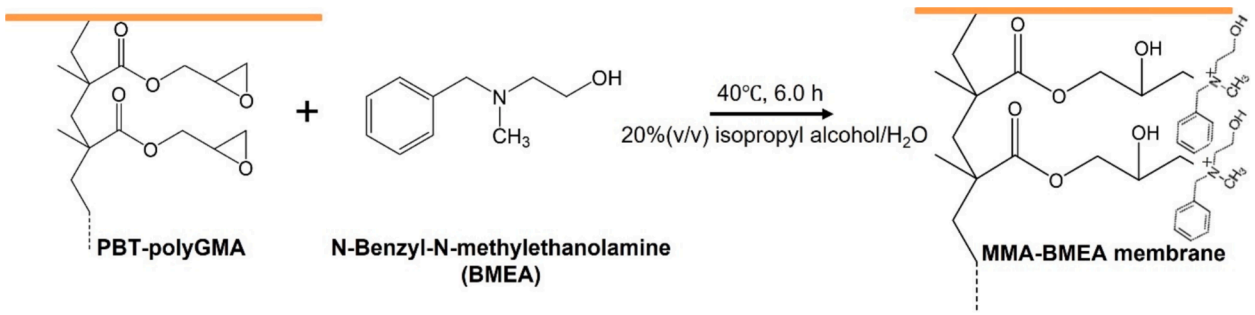

Fig. 2. Chemical reaction for coupling BMEA to polyGMA grafted PBT membranes.

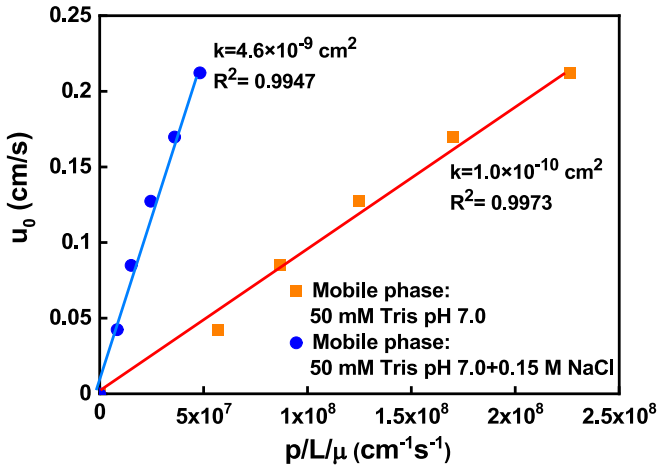

Fig. 3. Flow permeability of MMA-BMEA membrane in 50 mM Tris pH 7.0 with and without addition of 0.15 M NaCl (48 layers of MMA-BMEA membranes in a 10 mm diameter column). BMEA content in the ligand coupling reaction solution: 15% v/v.

obtained at 1.0 min RT were slightly lower than those obtained at 5.0 min, suggesting a slight diffusion limitation during adsorption to the grafted layer at the higher flow velocities. Under the same conditions, the $DBC_{10\%}$ of a commercial MMA Capto^{TM} adhere resin (0.24 mL CV) was measured to compare the performance of the MMA-BMEA membrane (**Fig. S4**). The results shown in **Table S1**, indicate that the $DBC_{10\%}$ of the MMA-BMEA membrane (30.8–38.5 mg/mL) was approximately 85% higher than that of the Capto^{TM} adhere resin (16.6–20.5 mg/mL) in the residence time range of 0.5 to 5.0 min at 0.15 M NaCl. This may be partly due to the higher ligand density and multilayer binding capabilities of the MMA-BMEA membrane, 150 μmol/mL versus 90–120 μmol/mL for the resin [41].

3.3. Direct capture of mAb from CHO supernatant by MMA-BMEA membrane

Having understood the performance of the MMA-BMEA membrane in terms of salt tolerance and protein binding and elution, the MMA-BMEA membrane was then applied to antibody purification. MMA resins have been used for mAb capture under physiological conditions, with reported $DBC_{10\%}$ generally less than 20 mg/mL at RT of 2.5–6.6 min with supernatant titers in the range of 0.4–1.69 mg/mL [24–26].

In previous work, a multimodal cation exchange membrane (MMA-MPCA membrane) was used to directly capture a mAb from CHO supernatant without pre-buffer exchange or dilution to reduce conductivity. However, this system required pH adjustment to 5.5 to bind the mAb [20], and the HCP clearance of 0.67 LRV was relatively low [20]. If the nonwoven MMA-BMEA exhibits a significant binding capacity for antibodies, it might play a key role in an all-membrane based process for mAb purification with greatly increased productivity and shorter overall process times compared to traditional platform processes utilizing resin column chromatography. Therefore, we first used polyclonal human IgG to evaluate the binding performance of the MMA-BMEA membrane for antibodies and then applied these results to the purification of a mAb from CHO cell culture using an all-membrane process.

3.3.1. Performance of MMA-BMEA membranes for bind-and-elute capture of polyclonal human IgG

Fig. 4 shows the equilibrium adsorption isotherm of polyclonal human IgG on the MMA-BMEA membrane, which was well fitted by the Langmuir model. The parameters resulted in a maximum binding capacity q_m of ~ 400 mg/g (133.3 mg/mL of dry membrane) and a dissociation constant K_d of 1.37 mg/mL (9.1 μM). The high equilibrium binding capacity results from the adsorption of IgG molecules throughout the grafted layers. The surface area of the nonwoven fibers used in this study is approximately 1 m^2/g of membrane. Monolayer binding of proteins to a surface results in approximately 5–6 mg of protein/m^2 of surface, therefore monolayer protein adsorption on the fibers would result in only 5–6 mg protein/g of fabric, a much lower value than the measured value of 400 mg of protein per g of membrane. The polyclonal IgG was absorbed by the MMA-BMEA membrane at pH 7.9, which is within the reported pI range of human IgG (7.1–8.2) [37,42,43]. This is not consistent with the rule in conventional anion-exchange chromatography that the binding pH should be higher than the pI of the target protein. One possible interpretation is that the hydrophobic and hydrogen bonding interactions are playing a critical role

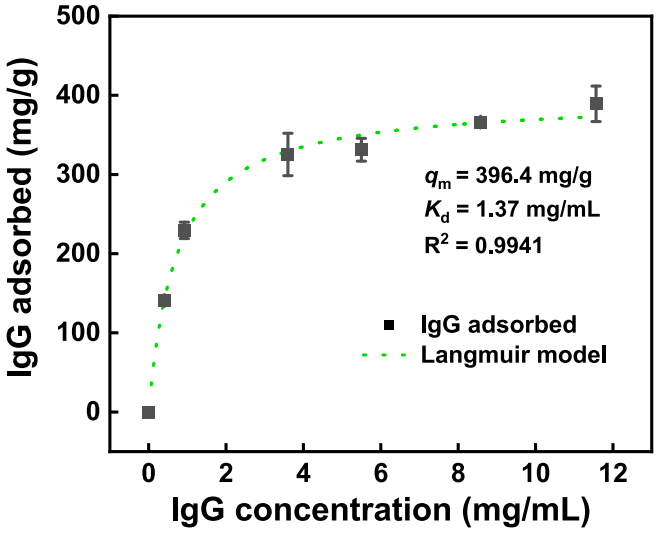

Fig. 4. Equilibrium adsorption isotherm of IgG binding to MMA-BMEA membrane. Initial IgG solution: 1.0 to 13.0 mg IgG/mL dissolved in pH 7.9 50 mM Tris-HCl with addition of 120 mM NaCl (≈14.5 mS/cm). The Langmuir isotherm was used to fit the experimental data.

in IgG binding under these conditions. Under flow conditions, the $DBC_{10\%}$ for polyclonal human IgG remains relatively constant around 40 mg IgG/mL from 1.0 min to 5.0 min RT as shown in Table 3 (A typical chromatogram at 1.0 min RT can be found in **Fig. S6**. Decreasing the RT from 5.0 min to 1.0 min resulted in only a 7.3% decrease in binding capacity due to diffusion limitations. Decreasing the residence time to 0.5 min resulted in a 22.6% decrease in binding capacity compared to the DBC at 5.0 min. This trend is similar to the $DBC_{10\%}$ trends found for BSA in **Table S1**. It should be noted that even though the binding capacity at 0.5 min is lower, the productivity of the binding step, defined in terms of mass of protein per mL resin per unit time is larger at the shorter residence time.

Membrane adsorbers will have to be used in several consecutive bind-and-elute cycles to handle the product loads in large-scale cell culture. To test the reusability of the MMA-BMEA membrane, five consecutive IgG bind and elute cycles with RT of 2.0 min were performed. Between each cycle, 0.5 M NaOH was used to clean and regenerate the membrane. The chromatogram in Fig. 5 shows five similar UV signal patterns for each IgG bind-and-elute cycle. Comparing the mass of eluted protein with the mass of bound protein during sample loading, 97.4 ± 2.8% of the bound IgG was eluted in each cycle, indicating a good reusability under these conditions. Many more cycles would have to be included in a more thorough investigation of reusability performance, but these preliminary results are an encouraging first step.

3.3.2. Determination of $DBC_{10\%}$ of MMA-BMEA membrane for mAb capture from CHO supernatant

The operating conditions for adsorption and elution of polyclonal IgG were employed for the study of mAb capture from a clarified CHO culture supernatant with a mAb concentration of 3.2 mg/mL, a pH of 7.45 and a conductivity of 11.9 mS/cm. The pI of the mAb is 7.6 – very close to the pH of the supernatant. To avoid overloading, the $DBC_{10\%}$ of the MMA-BMEA membrane was measured for mAb capture. After membrane equilibration, the CHO supernatant was loaded onto the membrane at 2.0 min RT, and the mAb concentration in each 0.5 mL effluent was measured to determine the $DBC_{10\%}$. The dotted curve in Fig. 6 represents the dimensionless mAb breakthrough curve with respect to the mAb concentration in the feed. It shows a $DBC_{10\%}$ of 59.2 mg/mL for mAb capture at a loading volume of 4.5 mL, confirming that mAb can be directly captured from the CHO supernatant by the MMA-BMEA membrane without prior pH and conductivity adjustment. In this case, the operating pH (7.9) here is higher than the pI (7.6) of the mAb, indicating that electrostatic attraction is likely involved in protein binding. The $DBC_{10\%}$ for the mAb is higher than for the polyclonal human IgG because much of the polyclonal IgG has a pI greater than 7.6, resulting in fewer negative charges that make it less prone to bind the BMEA ligand. Accordingly, a smaller loading volume of 4 mL was used in subsequent purifications to further reduce mAb breakthrough.

3.3.3. Optimization of residence time in the loading step

To investigate the effect of RT on mAb adsorption, recovery and HCP removal, RTs of 0.5, 2.0 and 5.0 min were used for the MMA-BMEA membrane capture process. The resulting chromatograms are shown in Fig. 7, and the corresponding purification results are listed in Table 4. The elution peak area increased slightly from 0.5 to 2.0 min RT, resulting in higher recoveries of 98.4% at 2.0 min RT and 99.6% at 5.0 min, compared to a somewhat lower recovery of 84.9% at 0.5 min RT. Since almost all bound mAb was eluted, this translates into ~ 15% less mAb binding at 0.5 min RT. This trend is consistent with the pure IgG binding at 0.5–5 min RT in Table 3. The lower mAb binding at 0.5 min RT can be attributed to diffusion limitations within the grafted layer. The HCP removal of ~ 0.5 LRV was stable at each RT, reflecting a small effect of flow rate on HCP clearance. Since many of the HCP in CHO are negatively charged, it is not surprising that the HCP LRV values are not very high (~0.5). The concentration of mAb is significantly larger than the total HCP concentration, and because of its larger size compared to host cell proteins, IgG can bind more strongly to the ligands on the membrane. Sample loading at 2.0 min RT was applied in subsequent studies.

Table 3
$DBC_{10\%}$ (IgG) of MMA-BMEA membrane at pH 7.9 and 120 mM NaCl. The initial IgG concentration is 3.2 mg/mL.

RT (min)	MMA-BMEA membrane
0.5	32.8 mg IgG/mL
1.0	39.3 mg IgG/mL
2.0	42.3 mg IgG/mL
5.0	42.4 mg IgG/mL

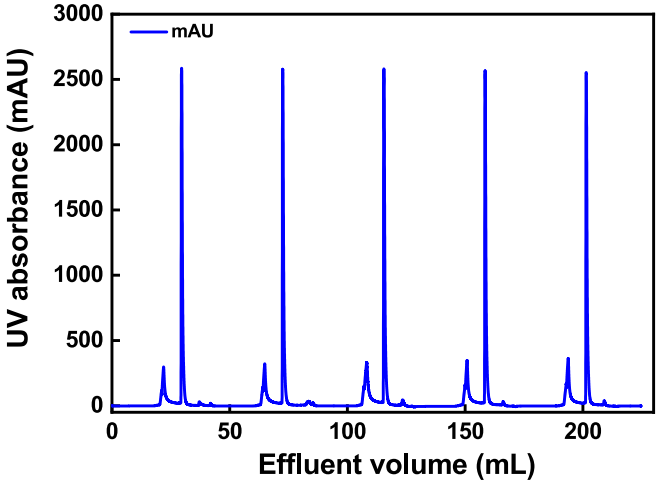

Fig. 5. Chromatograms of five consecutive human IgG bind-and-elute cycles at 2.0 min RT.

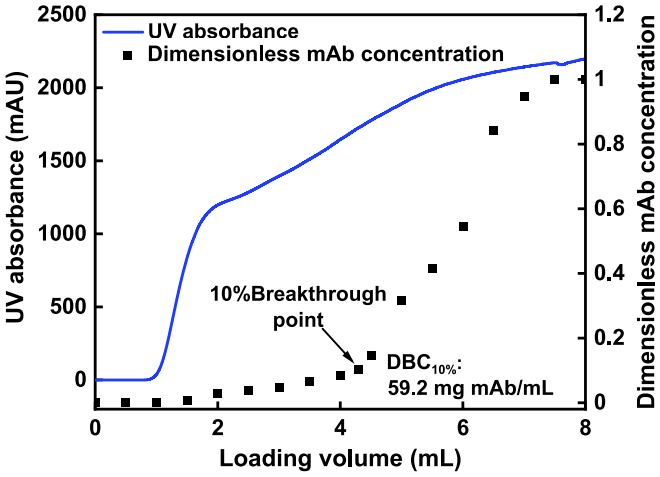

Fig. 6. Chromatogram of determination of $DBC_{10\%}$ for capturing mAb in CHO supernatant by MMA-BMEA membrane at 2.0 min RT.

3.3.4. Optimization of washing buffer

According to the results of Hirano et al. [44], the use of arginine as an additive in the wash step of Protein A chromatography improves HCP removal because it can weaken the charge interaction between mAb and HCPs. As a result, we introduced a membrane wash step with arginine concentration ranging from 50 to 125 mM after sample loading. The membrane separation performance was evaluated in terms of mAb recovery and removal of HCPs and aggregates. The chromatograms in

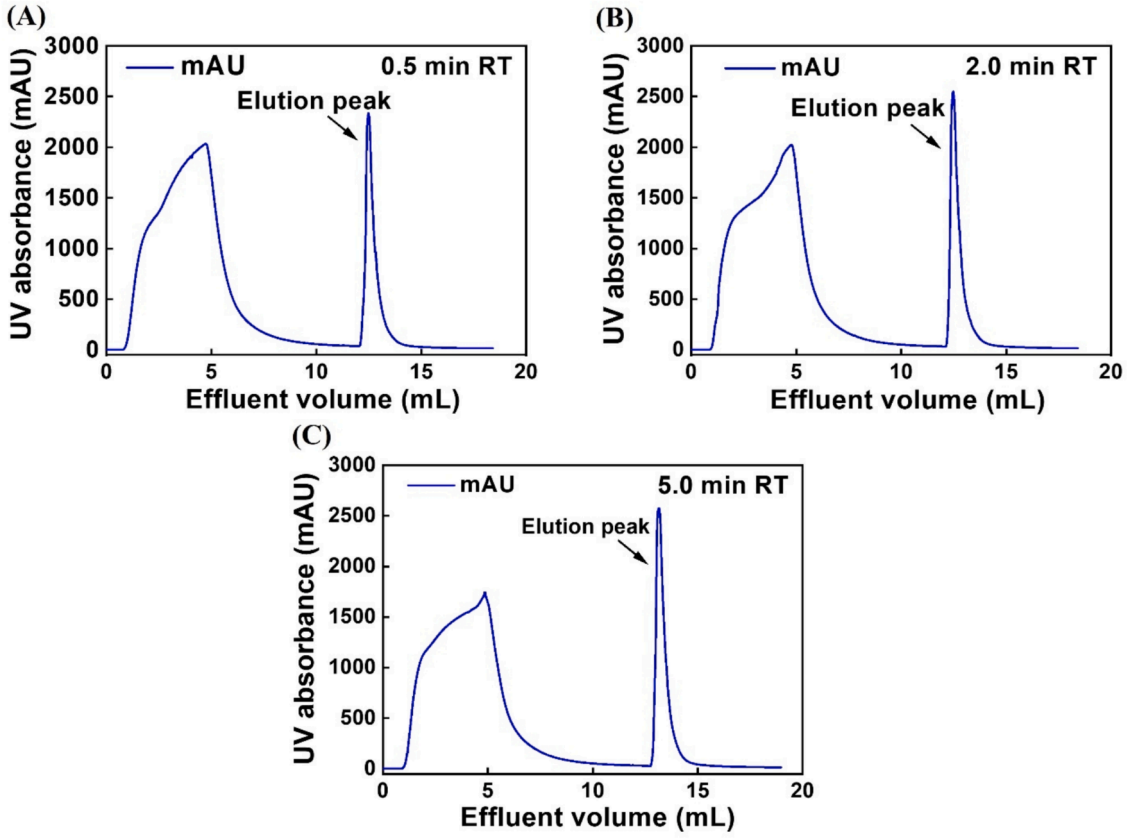

Fig. 7. Chromatograms of mAb capture by MMA-BMEA membrane at 0.5,2.0 and 5.0 min RT.

Table 4
Results of mAb recovery and HCP removal at 0.5, 2.0 and 5.0 min RT.

RT (min)	Recovery[1] (%)	HCP removal (LRV)
0.5	84.9	0.50
2.0	98.4	0.52
5.0	99.6	0.52

[1] Calculated as the mass ratio of the eluted mAb to the mAb applied in the loading solution.

Fig. S7 demonstrated an increase in UV absorbance with increasing arginine concentration during membrane washing, confirming the release of proteins by arginine. This caused a decrease in mAb recovery from 99.5% to 95.2%, an increase in HCP removal from 0.48 to 0.64 LRV and a slight decrease in aggregates from 3.7% to 3.4%. Since membrane washing with 87.5 mM and 125 mM arginine improved HCP and aggregate removal compared to no arginine washing, with little decrease in mAb recovery, a wash with 100 mM arginine was incorporated into the process.

3.3.5. *Elution pH optimization*

To further reduce the HCP level in the eluate, a two-step elution was performed at pH 4.5 and 4.0 and the resulting chromatogram is shown in Fig. 8**A**. A mAb recovery of 94.3% was obtained in the larger elution peak at pH 4.5 and the total HCP removal in the two steps is 1.0 LRV. This higher HCP removal compared to the pH 4.0 elution alone (~0.6 LRV in Table S2) suggests that some HCPs that bound more strongly to the BMEA ligand were retained on the membrane after the pH 4.5 elution. Meanwhile, the aggregate content in the pH 4.5 eluate was greatly reduced to 0.9% from the 5.4% in the supernatant. This is a significant improvement over the resulting aggregate content of 3.4–3.7% obtained by pH 4.0 elution alone (Table S2). This suggests that a large fraction of the aggregates was also retained after pH 4.5 elution. This was confirmed by the results of size exclusion HPLC, which showed that the pH 4.0 elution fraction had a high aggregate content of 81.1%. It also suggested that aggregates with larger number of charges and higher hydrophobicity are bound more strongly to the membrane than mAb monomer [45,46]. It is worth mentioning that the elution pH used for the MMA-BMEA membrane is generally higher than that used for most Protein A columns (<pH 4.0), which reduces the risk of forming aggregates.

In summary, the conditions for the MMA-BMEA product capture step includes: (1) supernatant loading to the membrane with no change in solution conditions, (2) 100 mM arginine wash for increased HCP and aggregate removal, and (3) elution at pH 4.5 to remove aggregates and HCP.

3.3.6. *All membrane process*

The high capacity of the MMA-BMEA nonwoven membrane for impurity removal and mAb recovery renders it a promising candidate for the development of a rapid and cost-effective all-membrane chromatographic process for mAb purification.

The membrane was used for the capture step in the complete process as described in Fig. 1, and the chromatogram is shown in Fig. 8**A**. The eluate at pH 4.5 from the MMA-BMEA membrane was adjusted to pH 3.6 and incubated for 1 h as a viral inactivation step. This was followed by a polishing step with an AEX-TEA membrane in flowthrough mode and a final polishing step with a cationic multimodal membrane (MMC-MPCA) in bind/elute mode, as shown in Fig. 1**.** A 2.0 min RT was used for supernatant loading and all other steps were done with 0.25 min RT. No buffer exchange or dilution was performed to adjust the conductivity of the supernatant.

Following virus inactivation, the pH of the solution was adjusted to pH 7.2 by the addition of 1.0 M Tris-HCl pH 8.0 and then filtered

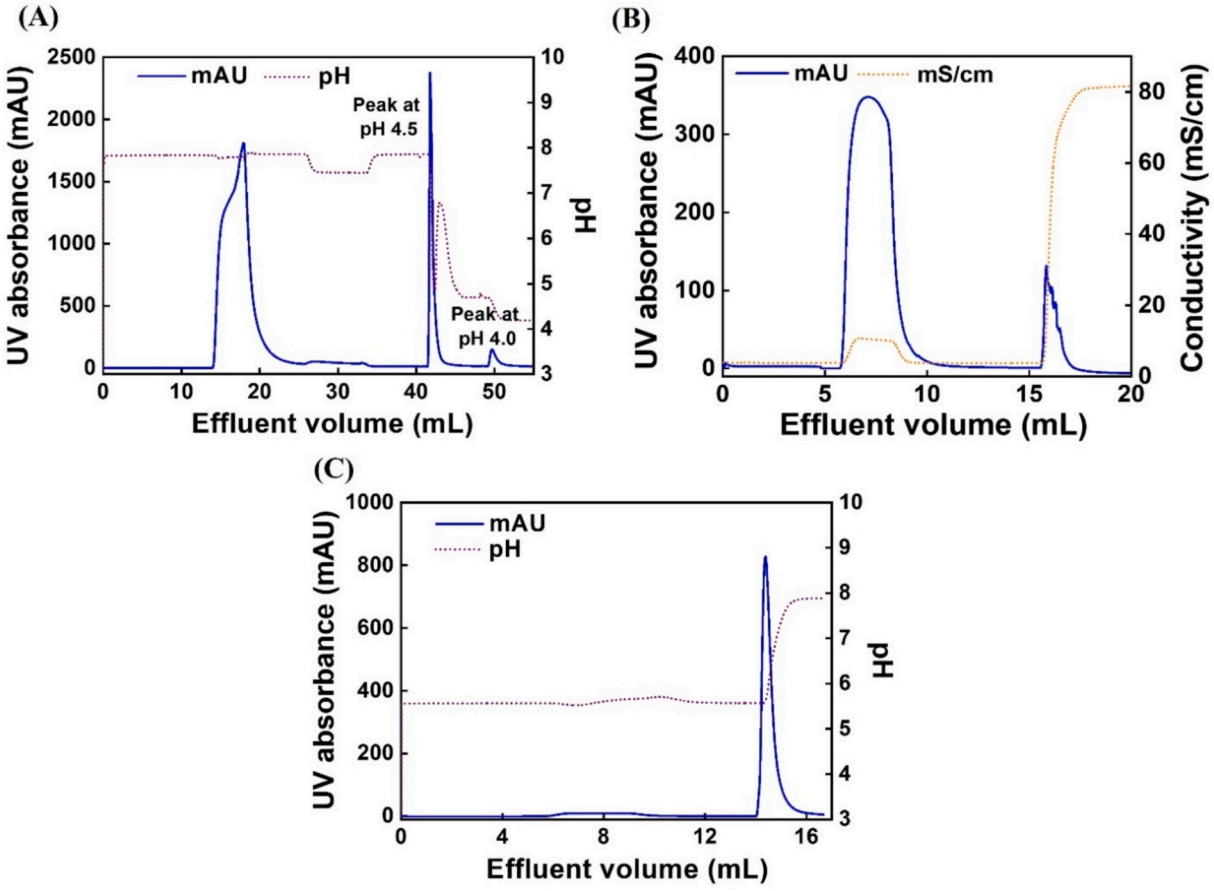

Fig. 8. Chromatogram of capturing mAb in CHO supernatant by MMA-BMEA membrane (A), subsequent polishing by AEX-TEA membrane (B) and final polishing by MMC-MPCA membrane (C). All steps were conducted at 0.25 min RT, except the sample loading at 2.0 min RT.

through a 0.22 μm microfiltration membrane. This step resulted in a 0.4 log reduction of HCP and a 0.3 log reduction of DNA. However, the aggregate content increased from 0.9% to 1.6%, likely due to the prolonged exposure at pH 3.6. The AEX-TEA membrane was then used as the first polishing process where the mAb with lower number of charges at pH 7.2 would flow through, while acidic impurities would be retained on the membrane. The resulting chromatogram, shown in Fig. 8**B,** presents a large and broad peak in the flow through fraction and a markedly smaller elution peak upon elution by 1.0 M NaCl. As demonstrated in Table 5, the membrane process yielded an excellent mAb recovery of 96.9% in the flow-through peak. The HCP, DNA and aggregate content were reduced from 12483.9 ppm in the feed to 1605.3 ppm (0.9 LRV), from 9.5 ppm to 0.052 ppm (2.3 LRV), and from 1.6% to 0.9%, respectively, thereby demonstrating a high mAb polishing performance.

Fig. 8**C** shows the chromatogram of the second polishing step, which was performed using the MMA-MPCA membrane in bind/elute mode. The pH of the flow-through fraction from the AEX-TEA membrane was adjusted to 5.5 by 0.5 M HCl prior to sample loading onto the MMA-MPCA membrane. This allows for the positively charged mAb to be adsorbed by the negatively charged ligands and other intermolecular forces. The bound protein was then eluted by 50 mM sodium phosphate pH 7.7 with the addition of 150 mM NaCl as it decreased the net positive charges on the mAb. A small and shallow peak is observed in the flow-through, while a considerably larger elution peak is evident, which should be mainly attributable to the eluted mAb, as a large fraction of impurities had been removed in the previous steps. The eluate exhibited

Table 5
Results of each step for mAb purification by nonwoven membranes.

	HCP (ppm)	HCP (LRV)	DNA (ppm)	DNA (LRV)	% Aggregates[1]	% Fragments[2]	% Recovery	Process time (min)	Productivity (g/L/h)[3]
CHO Supernatant	327367.6	——	994.7	——	5.4	0.8	——	——	——
MMA-BMEA Membrane (0.24 mL)	34062.5	1.0	17.8	1.8	0.9	Not detected	93.5	86.1	34.8
VI	12483.9	0.4	9.5	0.3	1.6	0.6	99.4	60.0	——
AEX-TEA Membrane (0.24 mL)	1605.3	0.9	0.052	2.3	0.9	0.1	96.9	40.0	72.0
MMC-MPCA Membrane (0.24 mL)	93.5	1.2	0.0068	0.9	0.4	Not detected	98.0	43.6	64.8

All steps were conducted in duplicate or triplicate and the average data was reported with less than 5% errors.
[1] Calculated according to the SEC chromatograms by HPLC in **Fig. S8**.
[2] Calculated according to the SEC chromatograms by HPLC in **Fig. S8**.
[3] Calculated as the mass of the eluted mAb per membrane volume divided by overall process time.

a high mAb recovery of 98.0%, and the purified mAb solution displayed a low level of impurities, with 93.5 ppm HCP (1.23 LRV), 6.8 ppb DNA (0.88 LRV), and 0.40% aggregates with no detected fragments (Table 5). The results demonstrated that the product met the generally accepted limits for mAb products: HCP < 100 ppm, DNA < 10 ppb, % aggregate < 1% [9]. This novel all membrane process yielded a very good overall recovery of 88.3% and an excellent overall impurity clearance of 3.5 LRV for HCP and 5.3 LRV for DNA, proving to be a promising alternative for efficient mAb purification. In future work, we will continue to optimize the purification process to further reduce residual HCPs below the current 93.5 ppm level.

3.3.7. Comparison of all-membrane process to platform process using resin column chromatography

To gain a deeper understanding of the potential benefits of the new all-membrane process for mAb purification, a comparison with a standard three-step resin chromatography process was carried out (shown in Fig. 1). In accordance with the manufacturer's recommendations for residence time in the resin columns (4–6 min), a 5.0 min RT was used in all resin steps to achieve optimal performance in terms of protein binding capacity and separation resolution [47,48]. We considered that increasing the flowrate in the column (shorter residence times) would reduce protein dynamic binding capacity, thereby lowering productivity. It could also adversely affect resolution by impacting the removal of HCP, aggregates, fragments and DNA.

The purification chromatograms are presented in Fig. 9, and the corresponding results are displayed in Table 6. The mAb capture step, conducted using the Eshmuno® Protein A column, obtained a high HCP removal of 2.3 LRV and DNA removal of 2.5 LRV. The aggregate content was reduced to 0.9%, which is identical to the level achieved by the MMA-BMEA membrane. The recovery of 90.6% is less than that of the MMA-BMEA membrane (94.3%). Following the virus inactivation, a strong cation exchange chromatography (Capto^{TM} S) was used for mAb polishing in bind/elute mode at pH 5.0. At this pH the mAb with positive charges can be absorbed by the negatively charged sulfonate. The elution was conducted at 0.4 M NaCl to reduce the charge interaction between the mAb and the ligand. This step removed part of the residual HCP, aggregates and DNA. As the residual HCP content of 150.9 ppm did not meet the typical requirement for mAb products (HCP < 100 ppm), a second polishing step by a strong anion exchange chromatography (Capto^{TM} Q) was introduced as in the typical mAb purification platform. The Capto^{TM} Q column was operated in flow-through mode at pH 6.5 to adsorb only acidic impurities with negative charges. Anion exchange was not employed as the first polishing process since the conductivity of the Protein A eluate is approximately 8–9 mS/cm, and this might not allow the adsorption of impurities in a flowthrough mode at a pH around 7. Since the anion exchange resin is not salt tolerant, the eluate from the preceding CEX column, which contained 400 mM NaCl, requires buffer exchange to reduce conductivity before being loaded on the AEX column. A salt tolerant anion exchange resin (Capto^{TM} adhere) was employed to avoid buffer exchange, but the resin exhibited a high degree of binding for the mAb (data not shown), rendering it unsuitable for implementation in flow-through mode. Nevertheless, the buffer exchange step performed with an ultra-centrifugal filter resulted in an approximate 10% increase in the aggregates. The high sheer speed of the centrifugation is the likely cause of the formation of aggregates, which should be largely mitigated in a real process scale using a crossflow filtration with an appropriate crossflow velocity. Further optimization of

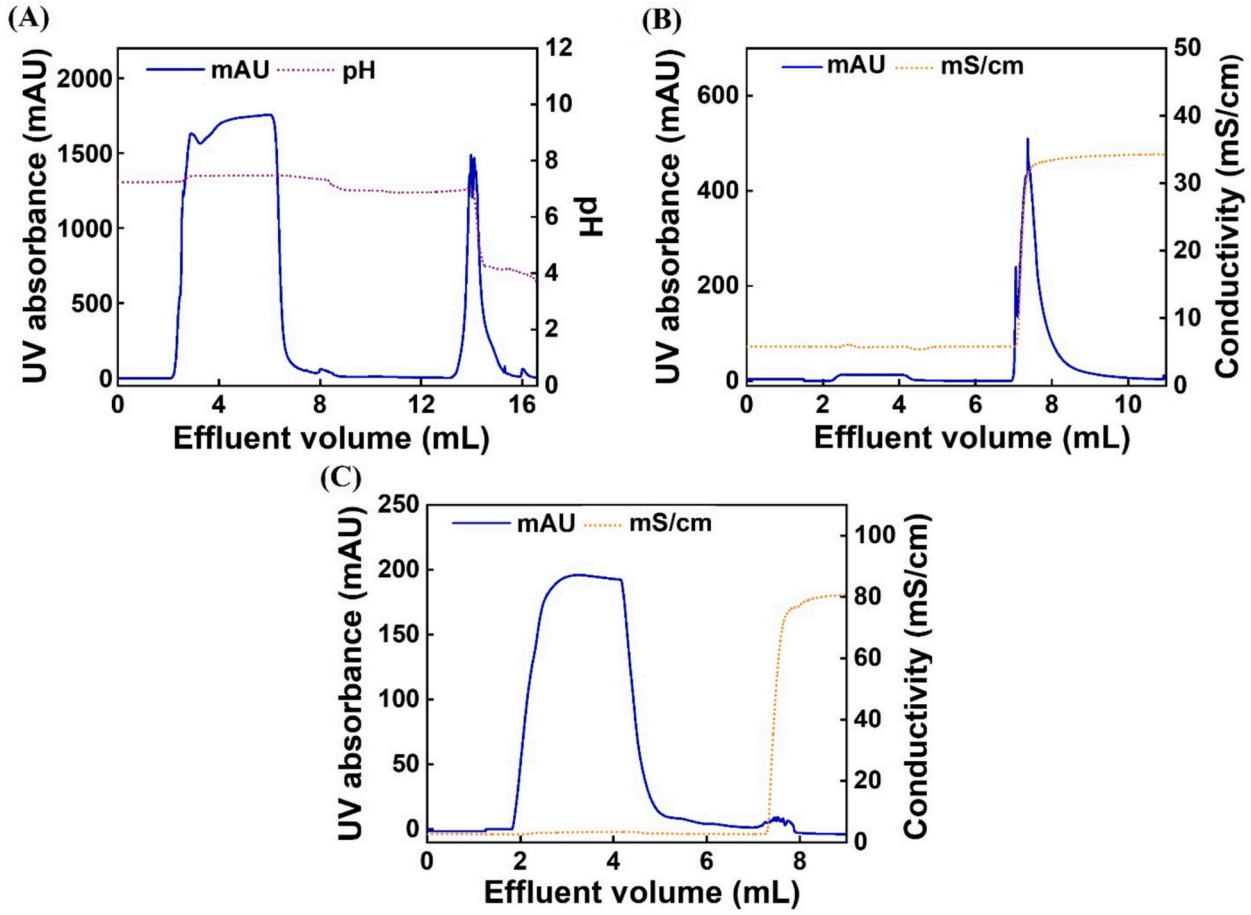

Fig. 9. Chromatogram of capturing mAb in CHO supernatant by Eshmuno® Protein A resin (A), subsequent polishing by Capto^{TM} S cation exchange resin (B) and final polishing by Capto^{TM} Q anion exchange resin (C). All steps were conducted at 5.0 min RT.

Table 6
Results of each step for mAb purification by resins.

	HCP (ppm)	HCP (LRV)	DNA (ppm)	DNA (LRV)	% Aggregates	% Fragments	% Recovery	Process time (min)	Productivity (g/L/h)
CHO supernatant	219785.1	–—	647.8	–—	5.4	0.8	–—	–—	–—
Protein A Resin (Eshmuno® Protein A, 0.28 mL)	959.2	2.3	2.2	2.5	0.9	Not detected	90.6	296.4	8.4
VI	386.4	0.4	0.5	0.6	1.0	1.0	97.8	60	–—
Cation Exchange Resin (Capto™ S, 0.25 mL)	150.9	0.4	0.01	1.6	0.1	0.1	95.8	225.0	11.6
Diafiltration (Centrifugal Filter 10 KDa MWCO)	147.0	~0	0.01	~0	10.0	Not detected	96.8	30	–—
Anion Exchange Resin (Capto™ Q, 0.25 mL)	20.4	0.9	Not detected	>1.0	15.3	Not detected	94.3	175.0	13.6

All steps were conducted in duplicate or triplicate and the average data was reported with less than 5% errors. The content of aggregates and fragments was measured with a Yarra SEC-2000 size exclusion chromatography column (300 mm × 7.8 mm) according to [37] and the corresponding chromatograms are shown in **Fig. S9**.

this buffer exchange step is beyond the scope of this study.

Despite the successful reduction of the final HCP content to 20.0 ppm, the strong anion exchange chromatography step was unable to effectively remove the aggregates. The overall process required 13.1 h to complete (Table 6), resulting in an overall HCP removal of 4.0 LRV, an overall DNA removal > 4.7 LRV, and overall recovery of 77.5%. In comparison, the all-membrane process, which required only 3.8 h, reduced the processing time by 71% with four times the productivity in the capture step and five to six times the productivity in the polishing steps (Table 5-6). If we replace anion exchange resin process with commercial anion exchange membrane for the final polishing step in the all resin process and it is operated at 10 membrane volumes/min (0.1 min RT), the overall process would require 10.2 h. In this case, the all membrane process reduced the processing time by 62.7%. Meanwhile, it resulted in a 14% higher overall recovery (88.3% vs. 77.5%) with fewer steps, comparable HCP and DNA clearance as well as fewer aggregates in the final product.

The production cost of these nonwoven chromatographic membranes is estimated to be between $100-$300/L of membrane, depending on the scale of production and labor costs. This would allow the membranes to be treated as single-batch disposable devices after several cycles of use, eliminating time-consuming and expensive cleaning and sanitization steps. The typical cost of Capto S and Capto Q ion exchange resins is approximately $3,000 per liter, while Eshmuno Protein A resin is around $10,000 per liter, and these are less likely to be used as single-use devices.

Buffer consumption has not been optimized for each process step, and a detailed cost comparison cannot be made. It should be noted that the buffers used in the equilibration, wash, and elution steps can be significantly reduced in the all-membrane process. For instance, the elution process can be completed in less than 10 membrane volumes (sufficient to collect the elution peak). Recent work in our laboratory has also shown that elution buffer consumption can be further reduced to less than 5 membrane volumes by designing flow distributors with much smaller dead volumes than the columns used to hold the membranes in this experiment. In the present case, the buffer consumption costs are comparable for both the all-membrane and all-resin processes. Nevertheless, even in this case, the shorter processing times of the all-membrane process allow for higher productivity, smaller process footprints, and more production flexibility – features that are well-known to reduce equivalent CO_2 emissions in biomanufacturing. A more comprehensive cost comparison of the all-membrane and column processes will be reported in future work.

4. Conclusions

Downstream processing of mAbs faces the challenges of increasing production efficiency while reducing costs. The mAb Protein A capture step is the costliest of the all the steps in the traditional mAb purification platform. Resin ion exchange columns used for further purification and polishing are also expensive and time-consuming. In this study, we proposed a strategy for purifying mAbs without using Protein A, that relies on nonwoven membrane chromatography for mAb capture, purification and polishing. For this purpose, an MMA-BMEA nonwoven membrane was developed using a pGMA UV-grafted PBT nonwoven as the base material. The excellent performance of the prepared membrane, including good salt tolerance, high flow permeability, good reusability and significantly superior binding capacity compared to the counterpart MMA resin, enabled direct capture of a mAb from a CHO supernatant at 0.5–5.0 min RT without pH or conductivity adjustments of the supernatant. Together with a recovery of 94.3% and excellent removal performance for HCP, DNA and aggregates, the MMA-BMEA provides a high-productivity approach for the capture of mAbs from CHO culture fluid.

Combined with the subsequent mAb polishing by AEX-TEA anion exchange nonwoven membrane and MMC-MPCA multimodal cation exchange nonwoven membrane, the three-step membrane chromatography process resulted in a significant reduction of impurities. The resulting mAb product adheres to common regulatory requirements, namely HCP < 100 ppm, DNA < 10 ppb, and % aggregates < 1%. Compared to the conventional resin process, employing Protein A column chromatography and two additional column ion exchange chromatography steps, the non-Protein A three-step membrane process exhibits a 71% shorter processing time, a 14% increase in overall recovery, and eliminates the need for diafiltration for buffer exchange. In this preliminary concept study, buffer consumption is higher in the all-membrane process due to overuse of the buffer solution in the elution steps, but this can be easily reduced by process optimization and using membrane flow cassettes with reduced dead volume. The new strategy proposed here for mAb purification based on all single-use chromatographic nonwoven membranes without affinity ligands has the potential to significantly enhance production efficiency and reduce costs in industrial antibody production.

CRediT authorship contribution statement

Jinxin Fan: Conceptualization, Data curation, Investigation, Writing – original draft, Writing – review & editing. **Joseph Lavoie:** Writing – review & editing. **Jacob LeBarre:** Data curation, Writing – review & editing. **Stefano Menegatti:** Writing – review & editing. **Behnam Pourdeyhimi:** Writing – review & editing. **Cristiana Boi:** Conceptualization, Supervision, Writing – review & editing. **Ruben G. Carbonell:** Conceptualization, Funding acquisition, Supervision, Writing – review & editing.

Declaration of competing interest

The authors declare that they have no known competing financial

interests or personal relationships that could have appeared to influence the work reported in this paper.

Acknowledgments

This research was funded by the William R. Kenan, Jr. Institute for Engineering, Technology and Science at NC State University and the Novo Nordisk Foundation (Grant # NNF19SA0035474). We gratefully acknowledge the support of the staff of the Golden LEAF Biomanufacturing Training and Education Center (BTEC).

Appendix A. Supplementary material

Supplementary data to this article can be found online at https://doi.org/10.1016/j.seppur.2025.132608.

Data availability

Data will be made available on request.

References

[1] G. Walsh, E. Walsh, Biopharmaceutical benchmarks 2022, Nat. Biotechnol. 40 (2022) (2022) 1722–1760, https://doi.org/10.1038/s41587-022-01582-x.
[2] A. Kirillova, A. Lado, N. Blatt, Application of monoclonal antibody drugs in treatment of COVID-19: a review, BioNanoScience 12 (2022) 1436–1454, https://doi.org/10.1007/s12668-022-00997-9.
[3] A. Puthenpurail, H. Rathi, S.M. Nauli, A. Ally, A brief synopsis of monoclonal antibody for the treatment of various groups of diseases, World J. Pharm. Pharm. Sci. 10 (2021) 14–22.
[4] S. Konstantinidou, A. Papaspiliou, E. Kokkotou, Current and future roles of biosimilars in oncology practice (Review), Oncol. Lett. 19 (2020) 45–51, https://doi.org/10.3892/ol.2019.11105.
[5] S. Nadar, B. Somasundaram, M. Charry, J. Billakanti, E. Shave, K. Baker, L.H. L. Lua, Design and optimization of membrane chromatography for monoclonal antibody charge variant separation, Biotechnol. Prog. 38 (2022) 15, https://doi.org/10.1002/btpr.3288.
[6] M. Rahman, J. Wang, H. Xia, J. Liu, Q. Bai, High capacity temperature-responsive affinity chromatography designed for antibody separation, Chem. Eng. J. 391 (2020) 123561, https://doi.org/10.1016/j.cej.2019.123561.
[7] S. Nadar, G. Shooter, B. Somasundaram, E. Shave, K. Baker, L.H.L. Lua, Intensified downstream processing of monoclonal antibodies using membrane technology, Biotechnol. J. 16 (2021) 11, https://doi.org/10.1002/biot.202000309.
[8] K. Gillette, M. Bisschops, M. Schofield, Development and optimization of multicolumn chromatography for mAb perfusion processes, J. Chem. Technol. Biot., 97 (2022) 2290–2296, https://doi.org/10.1002/jctb.6757.
[9] N. Kateja, D. Kumar, S. Sethi, A.S. Rathore, Non-protein A purification platform for continuous processing of monoclonal antibody therapeutics, J. Chromatogr. A 1579 (2018) 60–72, https://doi.org/10.1016/j.chroma.2018.10.031.
[10] M. Li, X. Zou, Q. Zhang, D. Lin, S. Yao, Binding mechanism of functional moieties of a mixed-mode ligand in antibody purification, Chem. Eng. J. 400 (2020) 125887, https://doi.org/10.1016/j.cej.2020.125887.
[11] Z. Li, Q. Gu, J.L. Coffman, T. Przybycien, A.L. Zydney, Continuous precipitation for monoclonal antibody capture using countercurrent washing by microfiltration, Biotechnol. Prog. 35 (2019) 8, https://doi.org/10.1002/btpr.2886.
[12] S. Grosshans, G. Wang, C. Fischer, J. Hubbuch, An integrated precipitation and ion-exchange chromatography process for antibody manufacturing: Process development strategy and continuous chromatography exploration, J. Chromatogr. A 1533 (2018) 66–76, https://doi.org/10.1016/j.chroma.2017.12.013.
[13] T. Kruse, M. Kampmann, I. Ruddel, G. Greller, An alternative downstream process based on aqueous two-phase extraction for the purification of monoclonal antibodies, Biochem. Eng. J. 161 (2020) 10, https://doi.org/10.1016/j.bej.2020.107703.
[14] I. Campos-Pinto, E. Espitia-Saloma, S.A. Rosa, M. Rito-Palomares, O. Aguilar, M. Arévalo-Rodríguez, M.R. Aires-Barros, A.M. Azevedo, Integration of cell harvest with affinity-enhanced purification of monoclonal antibodies using aqueous two-phase systems with a dual tag ligand, Sep. Purif. Tech. 173 (2017) 129–134, https://doi.org/10.1016/j.seppur.2016.09.017.
[15] V. Halan, S. Maity, R. Bhambure, A.S. Rathore, Multimodal chromatography for purification of biotherapeuties - a review, Curr. Protein Pept. Sci. 20 (2019) 4–13, https://doi.org/10.2174/1389203718666171020103559.
[16] K.A. Kaleas, M. Tripodi, S. Revelli, V. Sharma, S.A. Pizarro, Evaluation of a multimodal resin for selective capture of CHO-derived monoclonal antibodies directly from harvested cell culture fluid, J. Chromatogr. B 969 (2014) 256–263, https://doi.org/10.1016/j.jchromb.2014.08.026.
[17] H.R. Reese, X.Q. Xiao, C.C. Shanahan, G.A. Van den Driessche, D. Fourches, R. G. Carbonell, C.K. Hall, S. Menegatti, Novel peptide ligands for antibody purification provide superior clearance of host cell protein impurities, J. Chromatogr. A 1625 (2020) 13, https://doi.org/10.1016/j.chroma.2020.461237.
[18] X. Zou, Q. Zhang, H. Lu, D. Lin, S. Yao, Development of a hybrid biomimetic ligand with high selectivity and mild elution for antibody purification, Chem. Eng. J. 368 (2019) 678–686, https://doi.org/10.1016/j.cej.2019.03.014.
[19] J. Wang, E.W. Jenkins, J.R. Robinson, A. Wilson, S.M. Husson, A new multimodal membrane adsorber for monoclonal antibody purifications, J. Membr. Sci. 492 (2015) 137–146, https://doi.org/10.1016/j.memsci.2015.05.013.
[20] J. Fan, S.A. Sripada, D.N. Pham, Y.N. Linova, J.M. Woodley, S. Menegatti, C. Boi, R. G. Carbonell, Purification of a monoclonal antibody using a novel high-capacity multimodal cation exchange nonwoven membrane, Sep. Purif. Technol. 317 (2023) 123920, https://doi.org/10.1016/j.seppur.2023.123920.
[21] I.F. Pinto, M.R. Aires-Barros, A.M. Azevedo, Multimodal chromatography: debottlenecking the downstream processing of monoclonal antibodies, Pharm. Bioprocess., 3 (2015) 263–279, https://doi.org/10.4155/pbp.15.7.
[22] N. Yoshimoto, D. Itoh, Y. Isakari, A. Podgornik, S. Yamamoto, Salt tolerant chromatography provides salt tolerance and a better selectivity for protein monomer separations, Biotechnol. J. 10 (2015) 1929–1934, https://doi.org/10.1002/biot.201400550.
[23] M. Dileo, A. Ley, A.E. Nixon, J. Chen, Choices of capture chromatography technology in antibody manufacturing processes, J. Chromatogr. B 1068 (2017) 136–148, https://doi.org/10.1016/j.jchromb.2017.09.050.
[24] M. Toueille, A. Uzel, J.F. Depoisier, R. Gantier, Designing new monoclonal antibody purification processes using mixed-mode chromatography sorbents, J. Chromatogr. B 879 (2011) 836–843, https://doi.org/10.1016/j.jchromb.2011.02.047.
[25] J. Pezzini, G. Joucla, R. Gantier, M. Toueille, A.M. Lomenech, C. Le Senechal, B. Garbay, X. Santarelli, C. Cabanne, Antibody capture by mixed-mode chromatography: a comprehensive study from determinaton of optimal purification conditions to identification of contaminating host cell proteins, J. Chromatogr. A 1218 (2011) 8197–8208, https://doi.org/10.1016/j.chroma.2011.09.036.
[26] S. Maria, G. Joucla, B. Garbay, W. Dieryck, A.M. Lomenech, X. Santarelli, C. Cabanne, Purification process of recombinant monoclonal antibodies with mixed mode chromatography, J. Chromatogr. A 1393 (2015) 57–64, https://doi.org/10.1016/j.chroma.2015.03.018.
[27] J. Turnbull, B. Wright, N.K. Green, R. Tarrant, I. Roberts, O. Hardick, D. G. Bracewell, Adenovirus 5 recovery using nanofiber ion-exchange adsorbents, Biotechnol. Bioeng. 116 (2019) 1698–1709, https://doi.org/10.1002/bit.26972.
[28] S. Vogg, F. Pfeifer, N. Ulmer, M. Morbidelli, Process intensification by frontal chromatography: performance comparison of resin and membrane adsorber for monovalent antibody aggregate removal, Biotechnol. Bioeng. 117 (2020) 662–672, https://doi.org/10.1002/bit.27235.
[29] A.L. Hejmowski, K. Boenning, J. Huato, A. Kavara, M. Schofield, Novel anion exchange membrane chromatography method for the separation of empty and full adeno-associated virus, Biotechnol. J. 17 (2022) 10, https://doi.org/10.1002/biot.202100219.
[30] J. Osuofa, D. Henn, J.X. Zhou, A. Forsyth, S.M. Husson, High-capacity multimodal anion-exchange membranes for polishing of therapeutic proteins, Biotechnol. Prog. 37 (2021) 11, https://doi.org/10.1002/btpr.3129.
[31] J. Winderl, E. Neumann, J. Hubbuch, Exploration of fiber-base d cation exchange adsorbents for the removal of monoclonal antibody aggregates, J. Chromatogr. A 1654 (2021) 12, https://doi.org/10.1016/j.chroma.2021.462451.
[32] R.R. Davis, F. Suber, I. Heller, B.X. Yang, J. Martinez, Improving mAb capture productivity on batch and continuous downstream processing using nanofiber PrismA adsorbents, J. Biotechnol. 336 (2021) 50–55, https://doi.org/10.1016/j.jbiotec.2021.06.004.
[33] J. Schwellenbach, F. Taft, L. Villain, J. Strube, Preparation and characterization of high capacity, strong cation-exchange fiber based adsorbents, J. Chromatogr. A 1447 (2016) 92–106, https://doi.org/10.1016/j.chroma.2016.04.019.
[34] S.R. Dods, O. Hardick, B. Stevens, D.G. Bracewell, Fabricating electrospun cellulose nanofibre adsorbents for ion-exchange chromatography, J. Chromatogr. A 1376 (2015) 74–83, https://doi.org/10.1016/j.chroma.2014.12.010.
[35] J. Fan, E. Barbieri, S. Shastry, S. Menegatti, C. Boi, R.G. Carbonell, Purification of adeno-associated virus (AAV) serotype 2 from spodoptera frugiperda (Sf9) lysate by chromatographic nonwoven membranes, Membranes 12 (2022) 17, https://doi.org/10.3390/membranes12100944.
[36] S.M. Lemma, C. Boi, R.G. Carbonell, Nonwoven ion-exchange membranes with high protein binding capacity for bioseparations, Membranes 11 (2021) 181, https://doi.org/10.3390/membranes11030181.
[37] J. Fan, C. Boi, S.M. Lemma, J. Lavoie, R.G. Carbonell, Iminodiacetic acid (IDA) cation-exchange nonwoven membranes for efficient capture of antibodies and antibody fragments, Membranes 11 (2021) 15, https://doi.org/10.3390/membranes11070530.
[38] H.Y. Liu, P.V. Gurgel, R.G. Carbonell, Preparation and characterization of anion exchange adsorptive nonwoven membranes with high protein binding capacity, J. Membr. Sci. 493 (2015) 349–359, https://doi.org/10.1016/j.memsci.2015.06.002.
[39] H. Xie, Y. Gao, X. Zhan, D. Xie, Selection of quaternary ammonium groups for optimizing properties of water-soluble, photosensitive phenolic resins and study of their postcuring mechanism, J. Appl. Polym. Sci. 91 (2004) 2914–2922, https://doi.org/10.1002/app.13518.
[40] C. Yang, C. Ting, Preparation of quaternary ammonium resin by epoxy resin and tertiary amine and its electrodeposition properties, J. Appl. Polym. Sci. 49 (1993) 1019–1029, https://doi.org/10.1002/app.1993.070490608.

[41] J. Robinson, M.A. Snyder, C. Belisle, J. Liao, H. Chen, X. He, Y. Xu, S.M. Cramer, Investigating the impact of aromatic ring substitutions on selectivity for a multimodal anion exchange prototype library, J. Chromatogr. A 1569 (2018) 101–109, https://doi.org/10.1016/j.chroma.2018.07.049.
[42] D.D. Zhang, Z.Y. Guo, P.F. Guo, X. Hu, X.W. Chen, J.H. Wang, Polyoxometalate-coated magnetic nanospheres for highly selective isolation of immunoglobulin G, ACS. Appl. Mater. Inter. 10 (2018) 21876–21882, https://doi.org/10.1021/acsami.8b05334.
[43] Y.D. Luo, Q.L. Zhang, S.J. Yao, D.Q. Lin, Evaluation of adsorption selectivity of immunoglobulins M, A and G and purification of immunoglobulin M with mixed-mode resins, J. Chromatogr. A 1533 (2018) 77–86, https://doi.org/10.1016/j.chroma.2017.12.018.
[44] A. Hirano, T. Maruyama, K. Shiraki, T. Arakawa, T. Kameda, Mechanism of protein desorption from 4-mercaptoethylpyridine resins by arginine solutions, J. Chromatogr. A 1373 (2014) 141–148, https://doi.org/10.1016/j.chroma.2014.11.032.
[45] X.D. Zhang, T. Chen, Y.F. Li, A parallel demonstration of different resins' antibody aggregate removing capability by a case study, Protein Expr. Purif. 153 (2019) 59–69, https://doi.org/10.1016/j.pep.2018.08.011.
[46] P. Gagnon, R. Nian, J. Lee, L.H. Tan, S.M.A. Latiff, C.L. Lim, C. Chuah, X.Z. Bi, Y. S. Yang, W. Zhang, H.T. Gan, Nonspecific interactions of chromatin with immunoglobulin G and protein A, and their impact on purification performance, J. Chromatogr. A 1340 (2014) 68–78, https://doi.org/10.1016/j.chroma.2014.03.010.
[47] Eshmuno® A chromatography media. https://www.emdmillipore.com/Web-US-Site/en_CA/-/USD/ShowDocument-Pronet?id=201309.039, 2018 (accessed 23 December 2024).
[48] Purification of monoclonal antibodies using modern chromatography media and membranes. https://cdn.cytivalifesciences.com/api/public/content/digi-17015-pdf, 2015 (accessed 23 December 2024).